Journal of Nonlinear Optical Physics & Materials
Vol. 17, No. 1 (2008) 111–120

World Scientific
www.worldscientific.com

ESTIMATION OF THE COUPLING POWER PARAMETER OF FUSED COUPLED FIBERS

SAKTIOTO

Physics Department, Math and Science Faculty,
University of Riau, Pekanbaru, Indonesia
saktioto@yahoo.com

JALIL ALI

Institute of Advanced Photonics Science,
Science Faculty, Universiti Teknologi Malaysia,
81310 Skudai, Johor Bahru, Malaysia

MOHAMMED FADHALI

Physics Department, Faculty of Science,
Ibb University, Yemen

JASMAN ZAINAL

Institute of Advanced Photonics Science,
Science Faculty, Universiti Teknologi Malaysia,
81310 Skudai, Johor Bahru, Malaysia

Received 26 February 2008

Fiber couplers are widely used in telecommunications and industry as passive splitting power devices. The effective power coupling and transmission from one fiber to another is mainly determined by both the coupling length and the coupling coefficient. The coupling length can be calculated directly but the coupling coefficient depends upon the refractive index and the separation fiber axis. After the fusion processes of two SMF-28e® couplers, the refractive index is unknown due to a change in the radius of the fiber ($r_{\text{cladd}} < 40\,\mu$m and $r_{\text{core}} < 1.5\,\mu$m). The coupling coefficient range is obtained from a distribution of the coupling ratio and compared with the empirical formula, which also enables one to calculate the refractive index. In this experiment, the coupling coefficient in the range of 0.6–0.9/mm is calculated as a function of the separation fiber axis and the refractive index of the core and cladding. The result shows a good correlation between experimental results and theoretical calculation.

Keywords: Single mode fiber; coupling ratio; coupling length; coupling coefficient; refractive index.

1. Introduction

Single mode fiber (SMF) directional couplers made by the fusion elongation method have stimulated considerable interest in a variety of scientific fields over the last few years. Because of their promising potential for high-capacity data processing, SMF's are finding more usage as a transmission system.[1] Their unique properties also make them particularly interesting for a broad range of applications.

A fiber coupler produces a coupling coefficient that controls the effective power transmission to another junction. Even though the modeling of fiber coupling provides a good understanding of the coupling coefficient, experimentally, the determination of the coupling range is not clearly established. Various approaches have been investigated[2,3] regarding the fabrication of fiber-to-fiber couplers. However, there are not many publications on the coupling coefficient range corresponding to the refractive index of fiber couplers.

We report in this paper the results of a theoretical and experimental analysis of SMF couplers. Experimental measurements are presented in order to better describe the behavior and operation of fiber couplers as a fiber-optic system. The results of a weak-coupling theoretical approach are reported and found to agree rather well with the observed geometrical parameters of the coupler properties, coupling coefficient and refractive index. The refractive index is found to decrease after fusion.[4] The dependence of the coupling coefficient on the separation fiber axis and refractive index is also discussed.

2. Coupled Fiber and Coupling Coefficient

Photonic circuits for various applications can be realized if the required functional devices in integrated optics form are well-understood. A passive device is one in which there is no control over phenomena due to a wide range of parameter changes occurring at the same time during fusion, such as optical couplers. One important phenomenon occurring to optical couplers, as coupling of modes in space[5–7] which contributes power propagation along the coupled fiber, is the coupling coefficient. Even though the determination of the coupling coefficient for a practical directional coupler is difficult, by evaluating the channel waveguide modes and observing the fiber geometry, some calculation of the coupling coefficient range can be made.

Consider a coupled fiber splitting one source to become two transmissions as a Y junction. Two identical single mode coupled fiber 1×2 couplers[8] for power propagation at z axial length can be described as

$$\begin{aligned} P_2 &= P_0 \sin^2(\kappa z), \\ P_1 &= P_0 - P_2 = P_0[1 - \sin^2(\kappa z)] = P_0 \cos^2(\kappa z), \end{aligned} \tag{2.1}$$

where the power is split into fiber 1 and fiber 2. The axial length is periodically changed by $z = m\pi/\kappa; m = 0, 1, 2, \ldots$, for $m = 1$, $z = L_c = \pi/\kappa$.

L_c is the coupling length in millimeters. $P_2/(P_1 + P_2)$ and $P_1/(P_1 + P_2)$ are respectively defined as coupling power and transmission power. Both the power fraction is called the coupling ratio. A laser diode source of wavelength $\lambda = 1310\,\text{nm}$ is used and is related to the normalized frequency as

$$V = \frac{2\pi a}{[\lambda(n_1^2 - n_2^2)^{1/2}]}. \tag{2.2}$$

To show the wave propagation along two close fibers, the coupled modes equation can simply be taken[5] as

$$\begin{aligned} U_1(z) &= A(z)\exp(-i\beta_1 z), \\ U_2(z) &= A(z)\exp(-i\beta_2 z). \end{aligned} \tag{2.3}$$

Derivation of coupled mode equations for two waveguide systems is as follows:

$$\begin{aligned} \frac{dU_1}{dz} &= -i\beta_1 U_1 - iK_{12}U_1, \\ \frac{dU_2}{dz} &= -i\beta_2 U_2 - iK_{21}U_2. \end{aligned} \tag{2.4}$$

The first term on the right hand side of Eq. (2.4) is the usual propagation term and the second one is the coupling term. This equation propagates as a sine and cosine wave. Therefore, coupled mode solutions are

$$\begin{aligned} U_2(z) &= \left\{ \frac{\kappa}{\sqrt{(\kappa^2 + \delta^2)}} \right\} \sin(\kappa z), \\ U_1(z) &= \sqrt{(1 - U_2^2(z))}, \end{aligned} \tag{2.5}$$

where $\kappa = \sqrt{(\delta^2 + K_{12}K_{21})}$ is the coupling coefficient and δ, which is the phase mismatch factor, is defined as $(\beta_1 - \beta_2)/2$. Then the coupling coefficient[9] can be defined as

$$\kappa = \frac{(2\Delta)^{1/2}}{a} \frac{u^2}{V^3} \frac{K_o(wd/a)}{K_1^2(w)}, \tag{2.6}$$

where K_o and K_1 are the zeroth and the first order of the Hankel function, and u and w are respectively the normalized lateral phase constant and the normalized lateral attenuation constant. The symbol Δ is defined by $(n_1^2 - n_2^2)/2n_1^2$, a is the core radius and d is the separation fiber axis between cores.

At the same range position, κ can also be expressed as an effective power range for transmission to another fiber. The separation between two fibers is significant in the coupling coefficient, because it determines the effective power transmission to another fiber. To solve the coupling coefficient, a simple empirical relationship is used to calculate the value κ,[8] which is

$$\kappa = \left(\frac{\pi}{2}\right) \left(\frac{\sqrt{\delta}}{a}\right) \exp[-(A + Bd + Cd^2)], \tag{2.7}$$

with

$$A = 5.2789 - 3.663V + 0.3841V^2,$$
$$B = -7769 + 1.2252V - 0.012V^2,$$
$$C = -0.0175 - 0.0064V - 0.0009V^2,$$
$$\delta = \frac{(n_1^2 - n_2^2)}{n_1^2} \quad d = \frac{d}{a},$$

where n_1 and n_2 are the core and the cladding refractive index respectively.

3. Experimental Design and Operation

Figure 1 depicts the schematic of the SMF-28e® coupler fusion process. Two fibers are twisted once to have a tight coupling when pulled by a vacuum pump and heated by a H_2 gas flame torch at 1 bar. Two fibers are heated in the range of 800–1300°C, while the vacuum pump pulls the fibers to the left and the right side at a speed of 100 μm/s approximately. The operation of the coupler machine is to reach a certain coupling ratio by the fusion of fibers. The coupling ratio is detected by an InGaS photodetector, as shown on the monitor. Fusion fibers at the coupling region decrease from 75% until 85% in geometry size, where the previous core and the cladding diameter are respectively 8.2 μm and 125 μm.

4. Results and Discussion

In the fusion process, heating coupled fibers are not homogeneous in changing their structures and geometries at the coupling region. Their changes are complicated because refractive indices and fiber geometries are not linear. However, they tend to

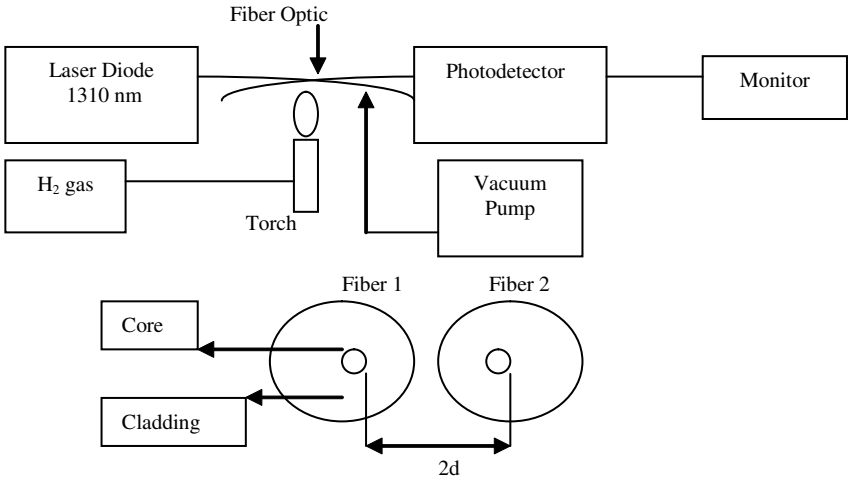

Fig. 1. The Schematic of the SMF-28e® coupler fusion process.

decrease exponentially along fibers from one edge to the center of the coupling region and again increase to one end. This also occurs to wave and power propagation along the coupling region. For simplicity, these results are concentrated only at the center of the coupling region with a homogeneous structure and geometry.

Measurements of fused coupling fibers' geometry are observed by a microscope. Using Eq. (2.1), the coupling length can be determined as shown in Fig. 2. The coupling ratio of x and (100-x) is the ratio of transmission and coupling power. In this calculation, κ is fixed at 0.903, the core and cladding refractive index as $n_1 = 1.4677$, $n_2 = 1.4626$, and the core radius $a = 4.1\,\mu$m. Figure 3 shows the coupling

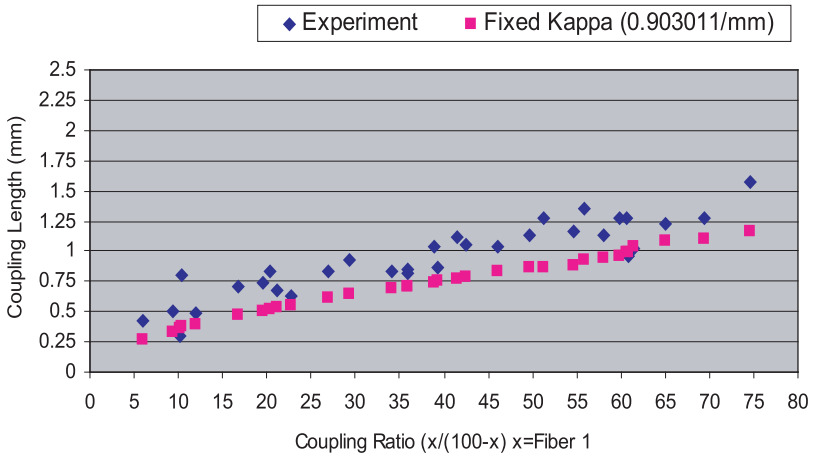

Fig. 2. Comparison of coupling lengths of SMF 28e®.

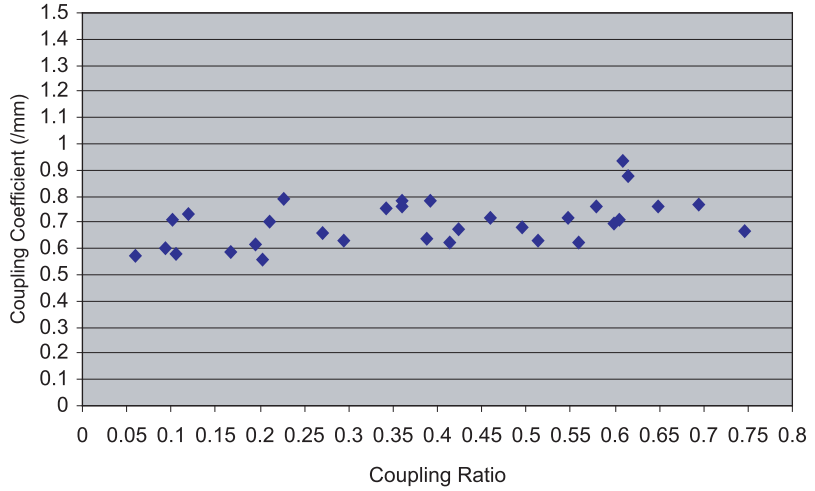

Fig. 3. Coupling coefficient of the SMF coupler.

coefficient of SMF-28e® versus the coupling ratio. Theoretical and experimental results agree that the coupling length increases over the coupling ratio due to the power propagation at the coupling region. It takes a longer time to reach complete coupling power, where the time is proportional to the coupling ratio.

The coupling length through measurement and fixed κ differ over a range of 0.25 mm. This is due to the separation of fibers, d which cannot be precisely measured. For calculation purposes, the value is set at 10 μm. Power loss during fusion also contributes to the coupling ratio range, however; for the calculation of fixed κ, it is not considered. Obtaining a good coupling ratio, the experimental result meets the power transmission at the coupling region with a larger coupling length than the calculation result. However, the coupling coefficient obtained from Fig. 3 is not constant. In the range of 0.6–0.9/mm, the coupling coefficient exists along the coupling ratio increase. This can be explained by assuming that the power transmission and coupling occur during fusion and fluctuates with some parameters, such as fiber twisting, fiber heating, and refractive index changes which cannot be controlled experimentally.

To analyze the coupling coefficient dependence on the refractive index, Fig. 4 describes two graphs of the refractive index of fibers before and after fusion. Before fusion, the refractive index is higher than after fusion. At the end of the fusion

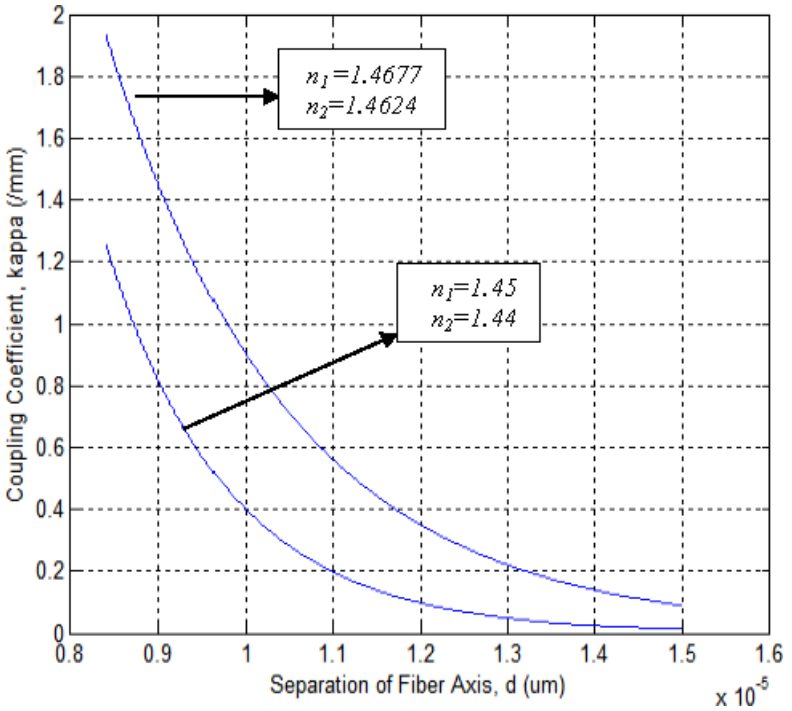

Fig. 4. Coupling coefficient of the SMF-28e® coupler heated by a torch flame.

process the coupling ratio, together with the refractive index of the core and cladding, changes.

Two graphs also representing a boundary of the fiber refractive index occurs when the fibers are fused at $n_1 = 1.45$ and $n_2 = 1.44$. It is expected that κ is in the range between two refractive index boundaries following Eq. (2.7). However, in Fig. 3, the coupling coefficient can be obtained through a separation fiber axis and κ is in the range of 0.6–0.9/mm. This corresponds to the axial separation fiber of 10–10.86 μm at $n_1 = 1.4677$ and $n_2 = 1.4624$. Comparing the cladding diameters experimentally obtained in the range of the coupling ratio of 1:75, where $2d =$ 18–35 μm, it is found that the separation between the two cores is $d = 9$–$17.5\,\mu$m.

In order to ensure that the refractive index after fusion is a boundary range, we set the mean separation of fibers $d = 10$–$10.86\,\mu$m. Figure 5 shows that δ decreases rapidly from 0.007 to 0.001 with a high gradient until the coupling coefficient approximately reaches 0.3. This explains why the refractive index will not attain $n_1 = 1.45$ and $n_2 = 1.44$ when the fibers are fused since the power transmission that keeps flowing along the fibers is high. Hence, in Fig. 4, the value of κ can agree with the requirement of the boundary conditions. By setting $\kappa = 0.9$–0.6/mm, the refractive index change $(n_1^2 - n_2^2)/n_1^2$ is in the range of 0.0086–0.092. Implicitly, this number is δ, the refractive index of both the core and the cladding after fusion. Analytical evaluation gives δ; n_2/n_1 is between 0.9956 and 0.9953. This is assuming that the ratio n_2/n_1 will proportionally decrease with κ. Thus, it is typically found that $n_2 = 1.4577$–1.4556 and $n_1 = 1.4640$–1.4623. Again, these values are within the coupling ratio of 1–75% of coupled fibers.

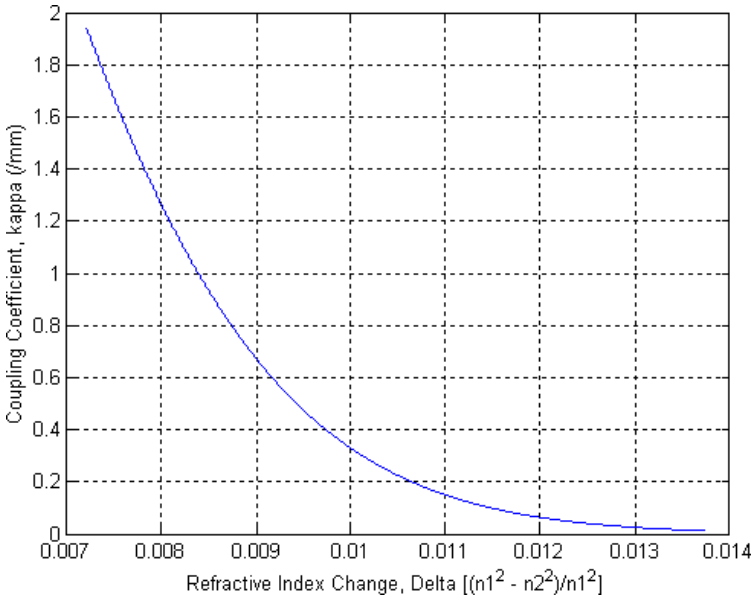

Fig. 5. The refractive index decreases due to fused fibers for $n_1 = 1.4677$–1.45, $n_2 = 1.4624$–1.44.

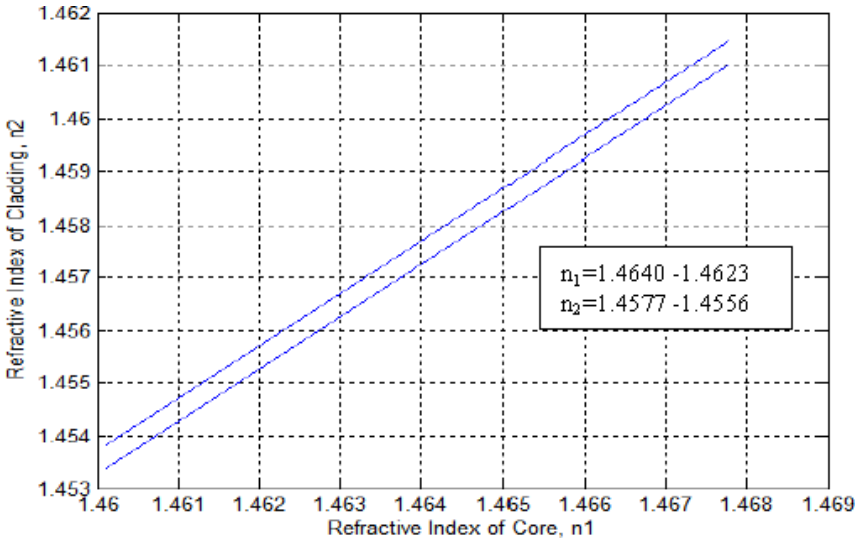

Fig. 6. Gradient of the refractive index for κ 0.9/mm (upper line) and 0.6/mm.

A gradient result of 0.9956 and 0.9953 in Fig. 6 represents the relation of the refractive index to the coupling coefficient at 0.9–0.6/mm. The slit range shown is narrow compared to small changes of the refractive index, by a factor of 10^{-3}. The value of κ extends widely, as expected from Eqs. (2.6) and (2.7). The upper ends of the two lines are the initial point of n_1 and n_2, which then decrease. The decreasing change of the refractive index from the initial point to the last together with $\Delta\kappa$ is 0.24–0.36% for the core and 0.31–0.45% for the cladding. The coupling coefficient depends on the refractive index, but not vice versa.

Comparing Figs. 4 and 5, the coupling coefficient is mainly affected by fiber separation by a factor of 10^{-1} rather than the refractive index, which is by a factor of 10^{-2}. Decrease of the refractive index reduces wave propagation along fibers in time and position, and the mode will travel widely to both claddings, whereas decrease of the core fiber separation affects whether the coupling ratio can be attained earlier and whether this effective power can be split readily to the Y junction.

According to Eq. (2.7), the value of κ depends on d by an exponential factor and δ rather than the refractive index of n_1 and $n_2 \cdot V$ and a are assumed to be constant. These parameters actually vary during the process, together with a wave number and propagation constant, due to changes in the fiber geometry. This description can be observed in Fig. 7. Since d is proportional to κ, increasing d at fixed δ will increase κ, although the separation of fibers is in a wide range. For a given core spacing, the coupling strength increases with the wavelength. This is due to the fact that the field extends deeper into the cladding and typical values are in the range of 0.1–2 mm^{-1} for core spacing in the range of 4–15 μm.[9] It also shows a

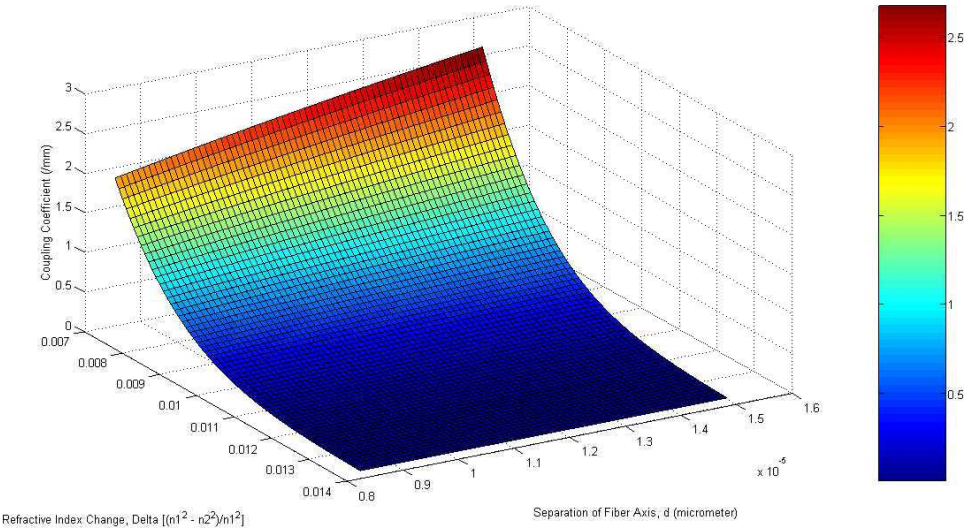

Fig. 7. Coupling coefficient of SMF-28e® for wide range of δ and d. $n_1 = 1.4677$–1.45 and $n_2 = 1.4624$–1.44.

strong decrease when the fiber core spacing increases, as expected from Eq. (2.6) by assuming that the interaction length is not considered with the radius of the curvature of the fibers and the wavelength. On the other hand, δ rapidly changes at higher d rather than at lower d. The refractive index difference between the core and the cladding is important because it dictates power coupling and transmission as the coupling coefficient is increased. However, if it occurs, the power and wave will radiate extensively into the cladding within a wider range. On the contrary, this is not the case with a single mode fiber. Therefore, it is necessary to obtain a higher coupling coefficient where both d and δ are optimized, although both parameters cannot be controlled easily during the fusion process, since fibers are heated continuously until the coupling ratio set is reached.

5. Conclusion

A coupling coefficient based on the distribution of the coupling ratio has been obtained. It is in the range of 0.9–0.6/mm, corresponding to determination of the refractive index by the empirical equation to the core and the cladding respectively as $n_1 = 1.4640$–1.4623 and $n_2 = 1.4577$–1.4556. The experimental results obtained are in good agreement with the empirical equation, and also in good correlation with the theory.

Acknowledgments

We would like to thank the Government of Malaysia, Universiti Teknologi Malaysia and the University of Riau, Indonesia, for their generous support for this research.

References

1. M. J. F Digonnet and H. J. Shaw, *IEEE J. Quantum Electron.* **18** (1982) 746–754.
2. A. Sharma, J. Kompella and P. K. Mishra, *J. Lightwave Technol.* **8**(2) (1990) 143–151.
3. I. Yokohama, J. Noda and K. Okamoto, *J.Lightwave Techn.* **5**(7) (1987) 910–915.
4. N. Kashima, *Passive Optical Components for Optical Fiber Transmission* (British Library Cataloging-in-Publication Data, Artech House Inc., 1995).
5. J. M. Senior, *Optical Fiber Communications*: *Principles and Practice*, 2nd edn. (Prentice-Hall, New Delhi, 1996).
6. H. A. Hauss, Series in Solid State Physics Electronics, in *Waves and Fields in Optoelectronics*, ed. Nick Holonyak, Jr. (Prentice-Hall, USA, 1984).
7. H. A. Hauss and W. Huang, *IEEE Proc.* **79**(10) (1991) 1505–1518.
8. R. P. Khare, *Fiber Optics and Optoelectronics* (Oxford University Press, India, 2004).
9. L. B. Jeunhomme and M. Dekker, *Single Mode Fiber Optics* (Principles and Applications, New York, 1990).